Surface Engineering of Tungsten Carbide Tool Material by Nano and Microcrystalline Diamond Coatings

Kaleem Ahmad Najar, Shah Aarif Ul Islam, and N. A. Sheikh

Abstract Diamond is generally accepted as a material with individual properties such as superlative hardness, low coefficient of friction and very high thermal conductivity. Synthetic diamond can be achieved in the form of thin and thick films using experimental chemical vapor deposition (CVD) methods. Cemented tungsten carbide (WC–Co) is the commonly used tool material with high hardness (~18 GPa) and high elastic modulus (~550 GPa) and, also compatible to the growth of synthetic diamond films. Presently, synthetic diamond coatings have been widely used on carbide cutting tools from long time to prevent the abrasive wear occurred on conventional tools. Based upon the size of the grains, synthetic diamond coatings are basically classified into nanocrystalline diamond (NCD) and microcrystalline diamond (MCD). In the work reported in the present chapter, smooth and adhesive thin NCD and MCD coatings were deposited on chemically treated tungsten carbide substrates using pre-determined process parameters in the hot filament chemical vapor deposition (HFCVD) method. Tungsten carbide with 6% Co is the mostly accepted grade of base material used for the successful growth of synthetic diamond films on its surface and, also to minimize the thermal residual stresses existing during the deposition and cooling down process between the interfaces of coating and substrate. Mostly, these thermal residual stresses are produced due to difference in thermal expansion coefficients between the coating and substrate. During deposition process, the process parameters such as methane concentration ($\%CH_4/H_2$) and chamber pressure were controlled automatically using pre-programmed recipe for the growth of NCD and MCD films. The structural characteristics and quality of the synthetic diamond films were confirmed using X-ray diffraction and Raman spectroscopy techniques, respectively. The surface morphology was studied using a high resolution scanning electron microscope (HRSEM) and atomic force microscope (AFM). Moreover, the hardness measurement of coatings were done using

K. A. Najar (✉) · N. A. Sheikh
Department of Mechanical Engineering, National Institute of Technology Srinagar,
Jammu & Kashmir, India
e-mail: najar.kaleem@gmail.com

S. A. U. Islam
Department of Physics, National Institute of Technology Srinagar,
Jammu & Kashmir, India

a Berkovich nanoindenter. After that, a comparative evaluation between these two types of coatings was done.

1   Introduction

Artificial diamond coatings are known to have exceptional tribological and mechanical properties (like better resistance to wear and tear, extraordinary hardness and low values of coefficient of friction) when subjected to sliding against several ceramic counter objects. Commonly, these synthetic diamond films are obtained through many CVD techniques using initial process parameters [1, 2].

Fundamentally, on the basis of grain size diamond films fabricated through CVD process has been classified as microcrystalline diamond (MCD) and nanocrystalline diamond (NCD). Coatings of NCD generally display nano-crystallinity comparable to ~3 µm thick coatings. The values of surface roughness and averaged grain size of NCD coating usually increase when there is an increase in the coating thickness [3]. NCD films are especially suitable for Tribological applications and are generally acquired by minimizing grain-size into nanometer-dimensions, but the internal thermal residual stresses within a coating can be increased with the decrease in grain size [4].

Owing to the higher amounts of sp^2-carbon content present in NCD films, these films have shown less adhesion quality on ceramic substrates in comparison to crystallized MCD films and this shows that the adhesive force will be more if the percentage graphitic-carbon phase is small near the substrate-coating interface [5]. The crystallinity and mechanical properties of NCD films will be highly affected owing to grain boundaries being large in number, which comprise of high amounts of graphitic-carbon [6]. In synthetic diamond growth, a well columnar grain pattern is witnessed every time that is a very significant factor to reveal morphology of the coated films [7]. The adhesive quality of diamond coatings is also significantly influenced by the film microstructure. Thus, the surface roughness (impurity), surface morphology and microstructure of a coating are the important factors for improving adhesive bond between substrate and diamond film [8, 9]. Many quantitative and qualitative experimental techniques can be used to investigate adhesion features of these coatings, such as dynamic scratch adhesion test and indentation test [10, 11]. The line-width of Raman peaks is directly correlated with both, growth rate of the film and inverse of the grain size, measured by X-ray method. Thus, the grain size of the coating is correspondingly directly related to the reciprocal of growth rate of the film [12].

In diamond films, there is development of two types of residual stresses; one is internal stress and the other is thermal stress (caused because of the coating and substrate having different thermal expansion coefficients). Thus, residual thermal

stresses are mostly affecting the adhesion strength of diamond films on the substrate [13]. The size of grains in coatings of diamond can well be increased from nanometer range to micrometer range by increasing the thickness of the coating and this will also lead to the increase in internal residual stress. Also, increasing the coating thickness improves the coating-resistance, de-lamination and capacity to bear load [14]. In general, the substrate-coating adhesive force can be improved by increasing the contact area [15]. For a large area diamond coated flat substrate the generated thermal strain can be calculated from Eq. (1), neglecting strain at the edges. Also, under plane stain conditions the resulting thermal stresses can be calculated from Eq. (2) [16].

$$\in_{th} = \sum_{T_S}^{T_R} [\alpha_S - \alpha_D] \Delta T \tag{1}$$

$$\partial_{th} = \frac{E_D \times \in_{th}}{(1 - V_D)} \tag{2}$$

In Eq. (1), α_D and α_S are the coefficients of thermal expansion of the coating and substrate, respectively, T_R, the room temperature and T_S, the growth temperature of coating. Also, E_D is the modulus of elasticity and V_D the Poisson ratio of the coating.

This chapter presents the studies on both MCD and NCD coatings that were deposited experimentally on chemically etched WC–Co substrates after maintaining the optimum process parameters. The surface characteristics, like crystalline quality and microstructure of these synthetic coatings were analyzed employing XRD, SEM and Raman techniques. Hardness property of each diamond coating was evaluated individually using Berkovich nanoindenter. Hence, the description of chemicals, materials, instruments and characterization techniques which are being utilized presently and also the technical details employed to perform the experiments involved, are explicitly discussed in the subsequent sections.

2 Materials and Methods

2.1 Chemical Etching Process

Ceratizit-CTF12A, with 6% Co, a cemented tungsten carbide (a candidate material for cutting tool) was chosen as a substrate with dimensions (10 mm × 10 mm × 3 mm) and ultrasonicated in ethyl alcohol to dislodge any impurities if present on the substrate surface. Since, on the surface of WC–6% Co substrate the presence of cobalt opposes the diamond film growth, as it encourages the graphitic-carbon formation, which in turn reduces the adhesive quality of the diamond coatings. Thus, prior to the deposition of high quality films of diamond on carbide substrates, chemical etching

Table 1 Pre-treatment of substrate surface procedure for growing MCD & NCD coatings [26]

S. no.	Procedural details	Chemicals	Remarks
1	Use soap solution to clean substrate	Detergent powder	Ultrasonic agitation
2	Rinse substrate in distilled H_2O	–	Dry using hot air blow
3	Degrease substrate	Acetone	Ultrasonic agitation
4	Rinse substrate in distilled H_2O	–	Dry using hot air blow
5	10 min chemical etching, after treatment with Murakami's reagent	Potassium Hydroxide, Potassium Ferricyanide	Ultrasonic agitation
6	Rinse substrate in distilled H_2O	–	Dry using hot air blow
7	10 s cobalt etching utilizing Caro's acid	Hydrogen Peroxide, Sulfuric Acid	Highly reactive solution
8	Rinse substrate in distilled H_2O	–	Dry using hot air blow
9	2 min ultrasonication	Ethanol	Ultrasonic agitation
10	10 min diamond seeding	Dispersed diamond seeds in (DMSO)	Ultrasonic agitation
11	Rinsing followed by 2 min cleaning	Isopropanol	Ultrasonic agitation
12	Dry using hot air blow	–	Load samples to chamber

is a very significant step. The whole steps of procedure for pre-treatment of surface for WC–6% Co substrate are listed in Table 1.

However, Fig. 1a, b show the XRD patterns of Co-cemented tungsten carbide sample before and after chemical etching process, respectively. The appearance of distinct (WC & Co) peaks explicitly depicts the removal of cobalt from the surface of tungsten carbide substrate by etching process, as seen in Fig. 1b. Surface cobalt was removed by Caro's acid and tungsten etching was done by Murakami reagent to form cavities on the surface due to which the strength of adhesion increases [17]. Figure 2a, b, c show surface morphologies of the cemented tungsten carbide (WC–6% Co) before treatment, and after treatment from Murakami Reagent and Caro's acid, respectively [18].

2.2   Hot Filament Chemical Vapor Deposition Process

The (HFCVD) hot filament chemical vapor deposition is a widely used deposition process to achieve various types of synthetic diamond coatings on carbides and ceramics for their industrial applications. Most of the tribological and mechanical
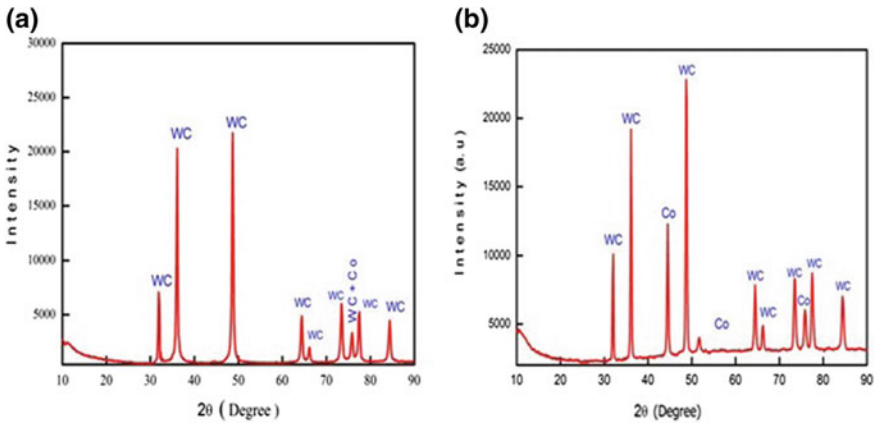
Fig. 1 XRD patterns of WC–Co substrate **a** prior to etching and **b** after etching [17]
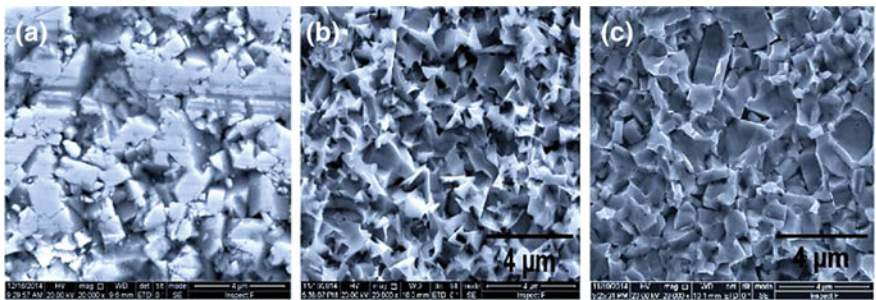

Fig. 2 Surface morphology of WC–Co sample **a** before treatment, and after treatment from **b** Murakami Reagent and **c** Caro's acid [18]

properties of these coatings are primarily affected by their crystallinity and grain size. Both these, grain size and crystalline quality of the diamond films are very important factors that are mostly controlled by methane percentage (%CH$_4$/H$_2$) ratio and pressure of the deposition chamber. For the growth of crystalline diamond the concentration of methane can be varied from 1 to 5% and the pressure of the chamber can be varied from 5 to 55 Torr, using initial pre-programmed recipe. Other parameters that influence the crystallinity and the rate of growth are, temperature of the substrate (700–900 °C) optimized, temperature of filament (1800–2200 °C) optimized and substrate to filament separation (1–4 cm) optimized.

In this work, HFCVD system (sp^3 Diamond Technologies, Model 650 series) was used to deposit synthetic films of diamond, as shown in Fig. 3. During deposition process, pressure of the chamber and concentration of methane were automatically controlled by mass flow controllers and throttle valve, respectively. In every experiment, a tungsten wire array (0.12 mm) were selected as hot filaments for the initiation of precursor gases (H$_2$ and CH$_4$) and the substrate-filament separation was
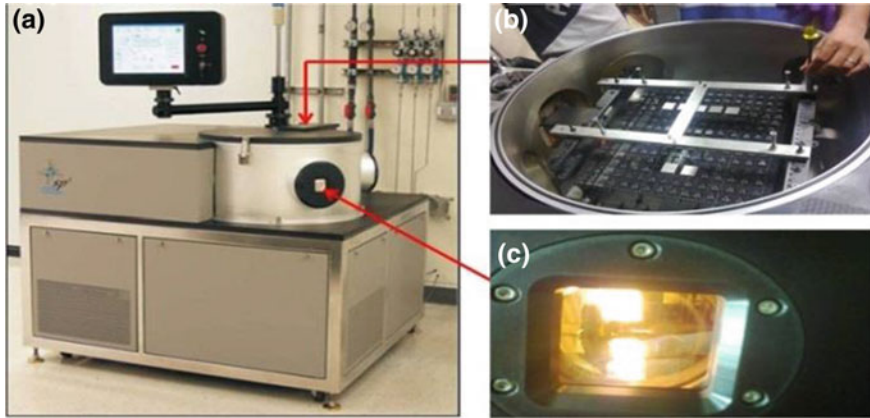
Fig. 3 **a** HFCVD instrumental setup, **b** Interior of deposition chamber and **c** quartz window view of the WC–Co substrates while diamond growth [18]

Table 2 Optimized growth/deposition parameters for NCD and MCD films [18]

Coating Type	Chamber Pressure (Torr)	CH_4/H_2 (%)	Filament temperature (°C)	Substrate temperature (°C)	Deposition Time (hrs.)	Coating Thickness (μm)
MCD	36	2	−2200	−850	3	−3
NCD	12	4	−2200	−850	3	−3

maintained at 1.5 cm. Hence, the growth parameters adopted in this experimental work for the optimized deposition of NCD and MCD coatings are stated in Table 2 [18]. After the deposition process, the toxic exhaust gases produced in the HFCVD chamber were diluted with nitrogen gas, which was used before and after the growth process to flush the chamber. The temperature of CVD chamber was retained at ~50 °C by means of a circulating water chiller and was made of aluminum with cooling channels.

3 Surface Characterizations Techniques

The microstructure and morphology of the surface of synthetic diamond coatings were observed by High Resolution Scanning Electron Microscope (HRSEM, Quanta 3D, FEI). The crystalline quality of the coatings was analyzed by the grazing incidence X-ray diffraction (XRD, GIXRD, PANalytical), having source wavelength $\lambda = 0.154$ nm and grazing angle of 3°. Structural characterization and stress state analysis was studied by Raman spectroscopy microscope (Alpha 300, WITec) having a laser wavelength of 488 nm.
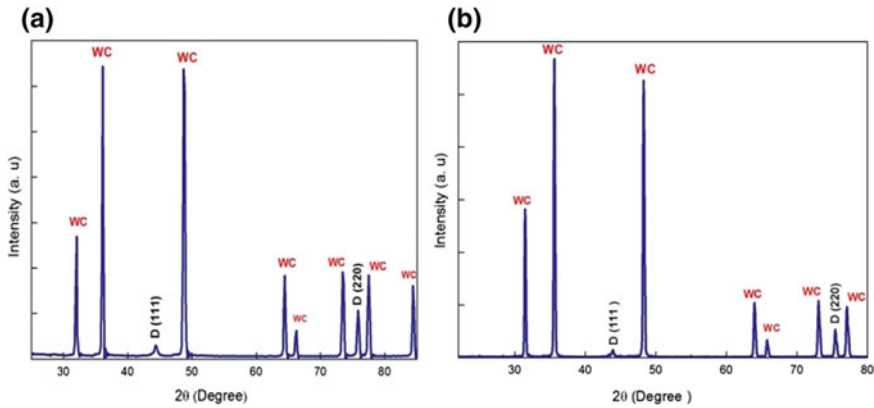
Fig. 4 XRD patterns of **a** MCD and **b** NCD coatings [17]

Generally, XRD technique is employed to reveal phase purity, phase type and the crystallographic structure of 2-D thin diamond films or 3-D bulk samples. Analysis of the XRD and Raman patterns revealed oriented crystalline and columnar growth along with high phase purity for both NCD and MCD coatings.

3.1 XRD Patterns of MCD and NCD Coatings

The X-ray diffraction patterns of NCD and MCD coatings are represented in Fig. 4a, b, respectively. Distinct and strong peaks of cubic diamond coating were observed at the diffraction angles of approximately 44° and 75.5° conforming to (111) crystal and (220) crystal planes, correspondingly for both these coatings, along with (WC) substrate peaks. These peaks reveal the high crystallinity of each diamond coating. It is clearly confirmed that the grain size of MCD coating is found more than NCD coating and also the grain size of carbide material is found more than each diamond coatings, due to the differences in their peak highest [17, 19].

3.2 Raman Spectroscopy of MCD and NCD Coatings

The crystallinity and chemical nature of diamond coatings were studied by using Raman spectroscopy technique. Thus, for the confirmation of diamond nature, a fundamental stress free Raman peak is shown by the diamond coating near about 1332 cm^{-1} [20]. Figure 5a, b show the Raman spectra of MCD and NCD diamond coatings, respectively. Here there is a shift towards higher side of the first order fundamental Raman peak which is focussed at 1333 cm^{-1}, indicates the residual
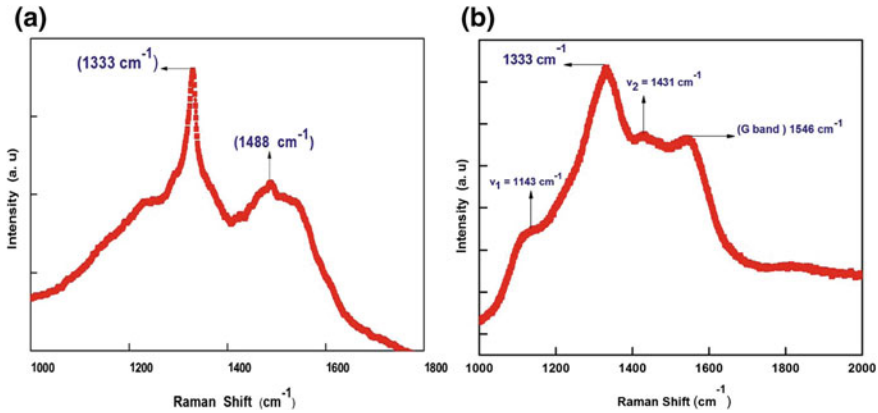
Fig. 5 **a** MCD coating and **b** NCD coating, Raman spectra [21] with kind permission from Elsevier

compressive stress being present in both these coatings. Owing to the different thermal expansion coefficients of coating and substrate, compressive residual stresses are produced [21], which can be estimated easily from the equation $\sigma = -0.348$ $(v_m - v_0)$ GPa for the un-split Raman peak, v_m, where $v_m = 1333$ cm^{-1} and $v_0 = 1332$ cm^{-1}. Hence, each deposited diamond film accommodates the compressive stresses of 0.348 GPa [22]. The other two peaks observed at $v_1 = 1143$ cm^{-1} and $v_3 = 1431$ cm^{-1}, represent the in-plane (C–H) characteristics and vibrational modes of (C=C) stretching, correspondingly. The presence of transployacetylene (TPA) chain along grain boundaries of the NCD coatings is the main source of these modes [23]. Also, the quality factor (Q) was calculated for the deposited diamond films by using the following formula [24].

$$Q = \{\frac{I_d}{I_{d+I_{glc}}}\} \times 100\% \tag{3}$$

where, I_d in Eq. (3) stands for intensity of the sharp diamond peak and I_{glc} stands for intensity of the graphitic-carbon broad peak. From Eq. (3), for NCD coating; $Q = \left\{\frac{1333\,\text{cm}^{-1}}{1333\,\text{cm}^{-1} + 1546\,\text{cm}^{-1}}\right\} \times 100\% = 46\%$.

3.3 Topography of the Surface of MCD and NCD Coatings

The microstructure, grain size and morphology of the diamond film surfaces were studied by HRSEM technique. Figure 6a, b, c show the HRSEM micrographs of NCD coating at different magnifications. The grain size on its surface is found to lie in the 0.2–0.6 µm range of morphology. In this aspect, the average grain size is calculated from the histogram of SEM micrograph as ~0.35 µm, represented in Fig. 6d. When
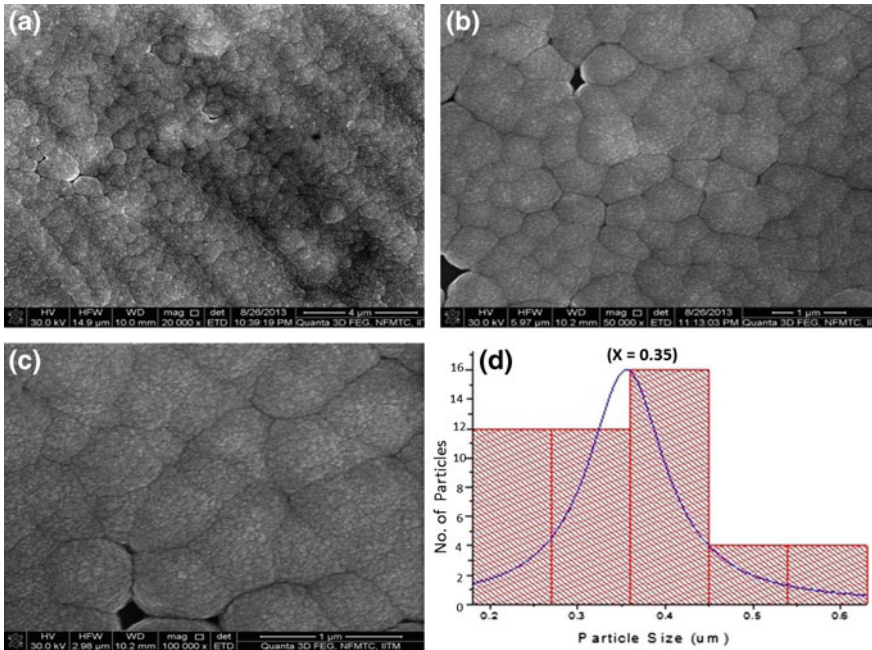
Fig. 6 **a**, **b**, **c** SEM micrographs of NCD coating at different magnifications, **d** Histogram of the SEM image [25]

the concentration of methane is increased from 2 to 4%, the development of secondary nucleation takes place that slows down the existing rate of growth of the grains, which results in a grain type having cauliflower like structure that is generally observed on NCD surface. Nano-features with normal grain growth were observed all over the surface and these are the important characteristics of thin nanocrystalline diamond coatings. Generally, on the surface of MCD film the grains with columnar structure and morphology of faceted form were observed. Similarly, Fig. 7a, b, c display the SEM micrographs of MCD coating at different magnifications, along with the grain size range lying in between 0.3 and 0.8 μm. The average grain size calculated from the histogram of its SEM image comes out to be ~0.57 μm, shown in Fig. 7d [3, 25]. Figure 8a, b display the typical cross-sectional morphologies of the NCD coatings and MCD coatings correspondingly, along with the coating and substrate thicknesses. The composition of both the surface coatings was verified by the energy dispersive analysis of X-rays spectroscopy (EDAX) technique, as shown in Fig. 9 [26].

Moreover, the AFM technique was employed in tapping mode for the surface imaging which reveals all the descriptions of phase and height imaging. Compared to HRSEM imaging, the AFM height imaging.
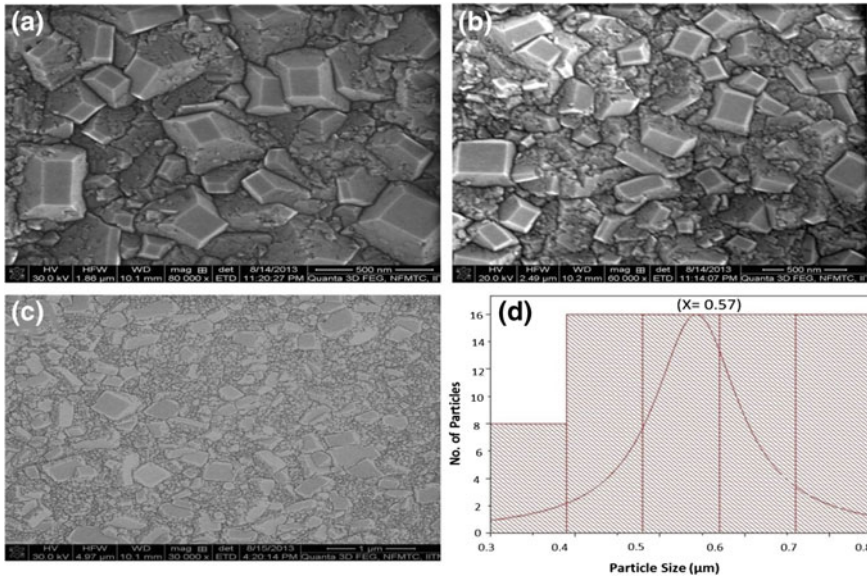
Fig. 7 **a**, **b**, **c** SEM micrographs of MCD coating at distinct magnifications, **d** Histogram of the SEM image [25]
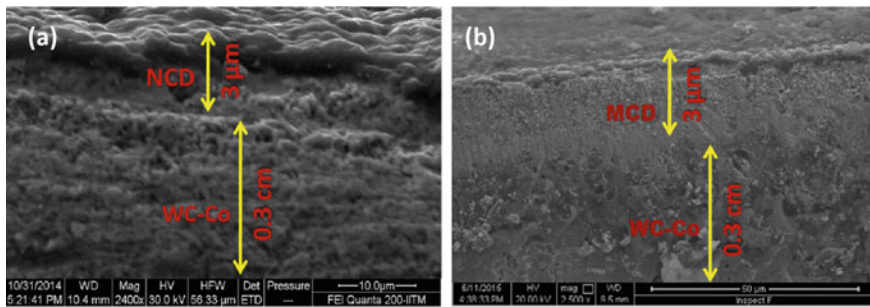

Fig. 8 Cross-sectional morphologies of **a** WC–Co/NCD and **b** WC–Co/MCD coating-substrate systems [26]

Provides much detailed and better topographical contrast. Here, the NCD and MCD coatings show different AFM phase images, as represented in Fig. 10a, b, correspondingly. During this AFM technique, similar areas of the MCD coatings and NCD coatings were scanned as in SEM technique and presented here. Therefore, Fig. 10a displays the 2D-AFM phase image of NCD coating at a scanning area of $2 \times 2 \ \mu m^2$. Small grain sizes with cauliflower type of smooth structures were visualized on the NCD surface and thus possess good tribological properties. Also, details of the height of these features are denoted by a color scale on the AFM height image and listed here. Similarly, for MCD coating, same area was scanned by AFM
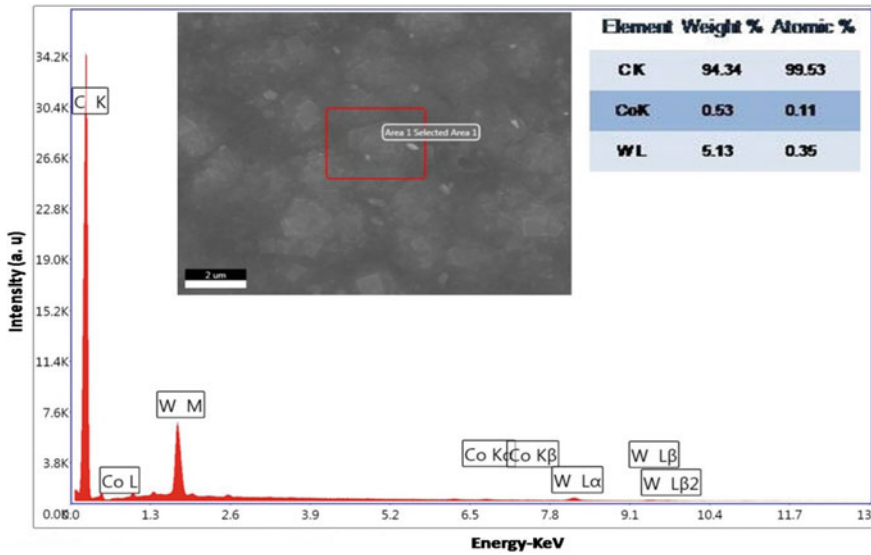
Fig. 9 Energy dispersive spectroscopy analysis (EDS) of NCD and MCD coating surfaces [26]

and represented here. Figure 10b displays the AFM phase image of MCD coating at scanning area of $2 \times 2\,\mu m^2$. Large grain sizes with faceted type of smooth structures were noticed on the surface of MCD, but the sharp features noticed on the MCD surface were unfavorable for them to be used in tribological applications [18].

3.4 Nano-Indentation and Hardness Measurement

Before Nano-indentation testing, the MCD and NCD coatings were polished by using a Tribometer and sliding for 2 h against Si_3N_4 pin. For these polished MCD and NCD coatings, Fig. 11a, b shows their load-displacement curves, respectively [26]. Thus, on each individual coating, four indentation tests were performed using Berkovich Nano-indenter. The average indentation depths for NCD coating and MCD coating were found to be ~79.75 nm and ~74.75 nm respectively and their excellent average hardness values were in the range of ~37–40 GPa and ~47–50 GPa, respectively. Also, the elastic modulus values of NCD coating and MCD coating were found to be ~1000 GPa and ~1100 GPa correspondingly, as calculated from the mathematical method by Oliver and Pharr [27].

(a)

ISO 25178		
Height Parameters		
Sq	0.143	V
Ssk	-0.146	
Sku	10.1	
Sp	0.872	V
Sv	2.64	V
Sz	3.51	V
Sa	0.106	V

(b)

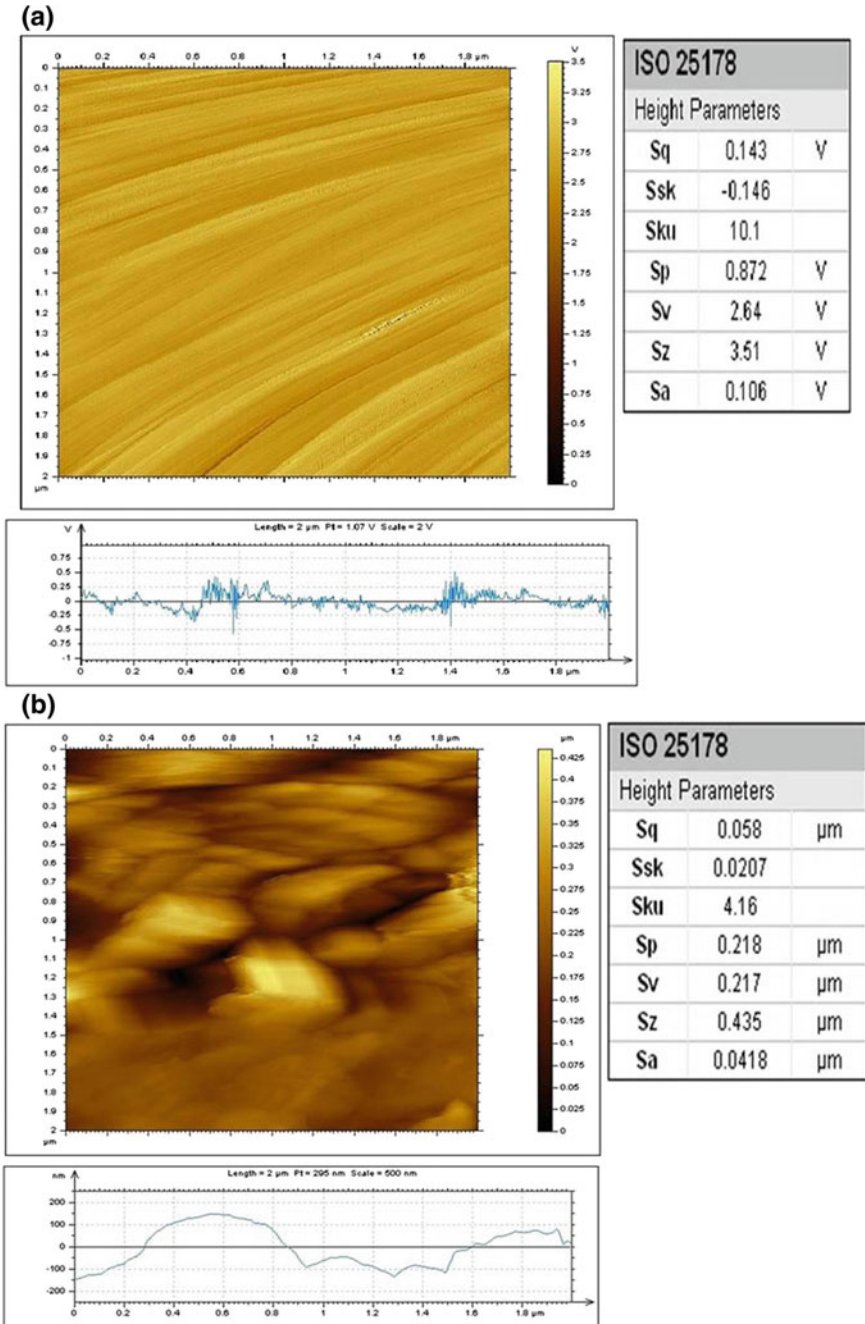| ISO 25178		
Height Parameters		
Sq	0.058	µm
Ssk	0.0207	
Sku	4.16	
Sp	0.218	µm
Sv	0.217	µm
Sz	0.435	µm
Sa	0.0418	µm

Fig. 10 AFM phase image ($2 \times 2 \ \mu m^2$) with height details, **a** NCD coating, **b** MCD coating [18]
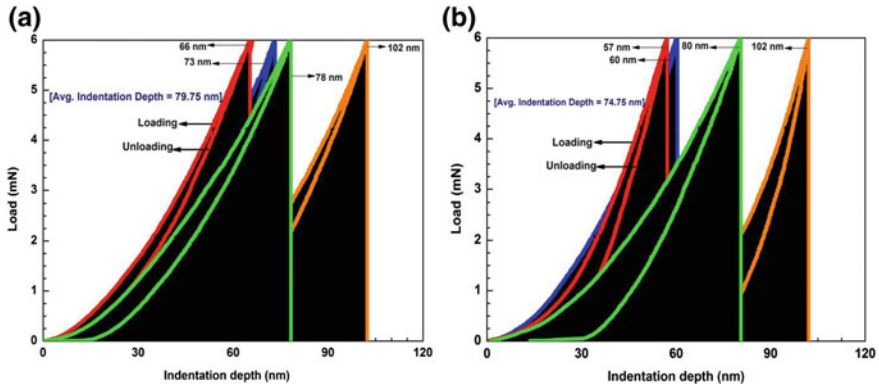
Fig. 11 Load-displacement curves equivalent to 4-indentations on **a** NCD and **b** MCD coatings [27] with kind permission from Cambridge University Press

4 Summary

I. The fabrication of crystalline and adhesive NCD and MCD coatings basically depends on the major controlling parameters (CH_4/H_2 ratio and pressure) in HFCVD chamber during initial pre-programmed recipe. Thus, synthetic diamond coatings deposited for 3 h. Enhancement of nucleation of NCD films was achieved at high methane concentration and low chamber pressure. Whereas, with low methane concentration and high chamber pressure enhanced the nucleation of MCD films. The increase in percentage of CH_4/H_2 ratio and decrease in chamber pressure, decreased the crystalline quality and grain size of the diamond coating.

II. Using HRSEM technique, the columnar structures of grains and faceted form of surface morphology were observed on the surface of MCD coating, whereas a cauliflower type of grain structure is generally seen on the surface of NCD coating.

III. Raman spectroscopy based study of synthetic diamond coatings confirmed the presence of trans-polyacetylene (TPA), and graphitic-carbon phases at the grain boundaries of the NCD coatings. The crystallinity of each diamond coating was confirmed using XRD method.

IV. The optimum diamond coating on the carbide substrate can be achieved by securing the optimum coating-thickness, grain-size of coating, and surface roughness of substrate before deposition. Moreover, increasing the thickness of diamond coating increases only load-bearing capacity of carbide material.

V. Hence, depositing smooth synthetic diamond coatings on carbide tools with optimum thickness, low friction coefficient, high hardness and good interfacial integrity will certainly be beneficial in many applications.

References

1. Erdemir, A., Fenske, G., Krauss, A., Gruen, D., McCauley, T., Csencsits, R.: Tribological properties of nanocrystalline diamond films. Surf. Coat. Technol. **120**, 565–572 (1999)
2. Sharma, N., Kumar, N., Dhara, S., Dash, S., Bahuguna, A., Kamruddin, M., et al.: Tribological properties of Ultrananocrystalline diamond film-effect of sliding counter bodies. Tribol. Int. **53**, 167–178 (2012)
3. Williams, O.A., Daenen, M., D'Haen, J., Haenen, K., Maes, J., Moshchalkov, V.V., Nesládek, M., Gruen, D.M.: Comparison of the growth and properties of ultrananocrystalline diamond and nanocrystalline diamond. Diam. Relat. Mater. **15**, 654–658 (2006)
4. Schwarzbach, D., Haubner, R., Lux, B.: Internal stresses in CVD diamond layers. Diam. Relat. Mater. **3**, 757–764 (1994)
5. Dumpala, R., Chandran, M., Kumar, N., Dash, S., Ramamoorthy, B., Ramachandra Rao, M.S.: Growth and characterization of integrated nano- and microcrystalline dual layer composite diamond coatings on WC–Co substrates. Int. J. Refract. Metals Hard Mater. **37**, 127–133 (2013)
6. Wiora, M., Brühne, K., Flöter, A., Gluche, P., Willey, T.M., Kucheyev, S.O., Van Buuren, A.W., Hamza, A.V., Biener, J., Fecht, H.J.: Grain size dependent mechanical properties of nanocrystalline diamond films grown by hot-filament CVD. Diam. Relat. Mater. **18**, 927–930 (2009)
7. Trava-Airoldi, V.J., Corat, E.J., Peña, A.F.V., Leite, N.F., Baranauskas, V., Salvadori, M.C.: Columnar CVD diamond growth structure on irregular surface substrates. Diam. Relat. Mater. **4**, 1255–1259 (1995)
8. Dauskardt, R.H., Lane, M., Ma, Q., Krishna, N.: Adhesion and debonding of multi-layer thin film structures. Eng. Fract. Mech. **61**, 141–162 (1998)
9. Salgueiredo, E., Almeida, F.A., Amaral, M., Neto, M.A., Oliveira, F.J., Silva, R.F.: A multilayer approach for enhancing the erosive wear resistance of CVD diamond coatings. Wear **297**, 1064–1073 (2013)
10. Bull, S.J., Berasetegui, E.G.: An overview of the potential of quantitative coating adhesion measurement by scratch testing. Tribol. Int. **39**, 99–114 (2006)
11. Buijnsters, J.G., Shankar, P., van Enckevort, W.J.P., Schermer, J.J., terMeulen, J.J.: Adhesion analysis of polycrystalline diamond films on molybdenum by means of scratch, indentation and sand abrasion testing. Thin Solid Films **474**, 186–196 (2005)
12. Ascarelli, P., Cappelli, E., Mattei, G., Pinzari, F., Martelli, S.: Relation between the HFCVD diamond growth rate, the line-width of Raman spectrum and the particle size. Diam. Relat. Mater. **4**, 464–468 (1995)
13. Woehrl, N., Hirte, T., Posth, O., Buck, V.: Investigation of the coefficient of thermal expansion in nanocrystalline diamond films. Diam. Relat. Mater. **18**, 224–228 (2009)
14. Qin, F., Chou, Y.K., Nolen, D., Thompson, R.G.: Coating thickness effects on diamond coated cutting tools. Surf. Coat. Technol. **204**, 1056–1060 (2009)
15. Saijo, K., Yagi, M., Shibuki, K., Takatsu, S.: Improvements in adhesive strength and cutting performance of diamond-coated tools. Surf. Coat. Technol. **47**, 646–653 (1991)
16. Sheikh-Ahmad, J., Chipalkati, P.: Effect of cutting edge geometry on thermal stresses and failure of diamond coated tools. Proc. Manufact. **30**, 1–12 (2015)
17. Najar, K.A., Sheikh, N.A., Dina, S., Shah, M.A.: Effect of CVD-diamond coatings on the tribological performance of cemented tungsten carbide substrates. J. Tribol. **9**, 1–17 (2016)
18. Najar, K.A., Sheikh, N.A., Shah, M.A.: Enhancement in tribological and mechanical properties of cemented tungsten carbide substrates using CVD-diamond coatings. Tribol. Ind. Faculty Eng. **39**(1), 20–30 (2017)
19. Dumpala, R., Kumar, N., Kumaran, C.R., Dash, S., Ramamoorthy, B., Ramachandra Rao, M.S.: Adhesion characteristics of nano- and micro-crystalline diamond coatings: Raman stress mapping of the scratch tracks. Diamond Relat. Mater. **44**, 71–77 (2014)
20. Prawer, S., Nemanich, R.J.: Raman spectroscopy of diamond and doped diamond. Philos. Trans. R. Soc. Lond. A **362,** 2537–2565 (2004)

21. Gunnars, J., Alahelisten, A.: Thermal stresses in diamond coatings and their influence on coating wear and failure. Surface Coat. Technol. **80**, 303–312 (1996)
22. Chandran, M., Kumaran, C.R., Gowthama, S., Shanmugam, P., Natarajan, R., Bhattacharya, S.S., Ramachandra Rao, M.S.: Chemical vapor deposition of diamond coatings on tungsten carbide (WC–Co) riveting inserts. Int. J. Refract. Metals Hard Mater. **37**, 117–120 (2013)
23. Kuzmany, H., Pfeiffer, R., Salk, N., Günther, B.: The mystery of the 1140 cm^{-1} Raman line in nanocrystalline diamond films. Carbon **42**, 911–917 (2004)
24. Ali, N., Neto, V.F., Mei, S., Cabral, G., Kousar, Y., Titus, E., Ogwu, A.A., Misra, D.S., Gracio, J.: Optimisation of the new time-modulated CVD process using the Taguchi method. Thin Solid Films **469–470**, 154–160 (2004)
25. Najar, K.A., Shah, M.A., Sheikh, N.A.: Integrity of CVD-Diamond coatings on cemented tungsten carbide substrate: mathematical analysis carried out for calculating the force of De-lamination and load bearing capacity of coating-substrate system. Elixir Nanotechnol. **90**, 37463–37467 (2016)
26. Najar, K.A., Sheikh, N.A., Butt, M.M., Shah, M. A.: Mathematical analysis carried out on the study of compatibility, De-lamination and load-bearing capacity of synthetic diamond coatings deposited on tungsten carbide composites. J. Nanotechnol. Mater. Sci. (OMMEGA Publishers), **6**(1), 10–16 (2019)
27. Oliver, W.C., Pharr, G.M.: Improved technique for determining hardness and elastic modulus using load and displacement sensing indentation experiments. J. Mater. Res. **7**, 1564–1583 (1992)